Hollow central radiation profiles and inverse sawtooth-like crashes in ASDEX Upgrade plasmas with central wave heating

A. Gude, M.Maraschek, C. Angioni, J. Stober and the ASDEX Upgrade Team

Max-Planck-Institut für Plasmaphysik, Garching, Euratom Association, Germany

Hollow soft X-ray radiation (SXR) profiles have been observed in ASDEX Upgrade in discharges with high enough central Electron Cyclotron Resonance Heating (ECRH) power, both in ECRH only as well as in ECRH and Neutral Beam Injection (NBI) heated plasmas. In such discharges, crashes have been observed, where the SXR profiles relax regularly from hollow to approximately flat. In the following we call these crashes, with central increase of SXR, inverse crashes (IC).

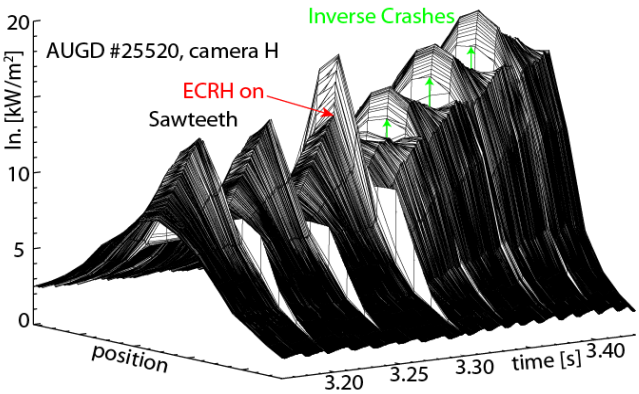

Figure 1: Time evolution of SXR profile (line integrals, time averaged over 200 ms) for an H-Mode discharge when central ECRH is switched on. The strong increase during the late phase of the last sawtooth cycle is due to the rise of central T_e. The ICs are followed by a further increase in radiation correlated to an increase in T_e.

The SXR diagnostic at ASDEX Upgrade [1] measures line integrated total radiation power in the photon range above ≈ 1 keV with pinhole cameras. Usually Bremsstrahlung is dominant, i.e., the profiles of electron density (n_e), electron temperature (T_e) and Z_{eff} determine the radiation. In case of metal walls, like the W wall in ASDEX Upgrade [2], line radiation from heavy impurities, which are not fully ionized in the plasma centre, can contribute strongly, or even dominate, the total SXR radiation. The camera (H) used throughout this paper is at the low field side below the magnetic axis. Discharges in this paper have I_p=1MA, $|B_t|$= 2.42-2.5T, q_{95}=4.5-4.7 and line averaged central densities around $8 \cdot 10^{19}$ m^{-3}.

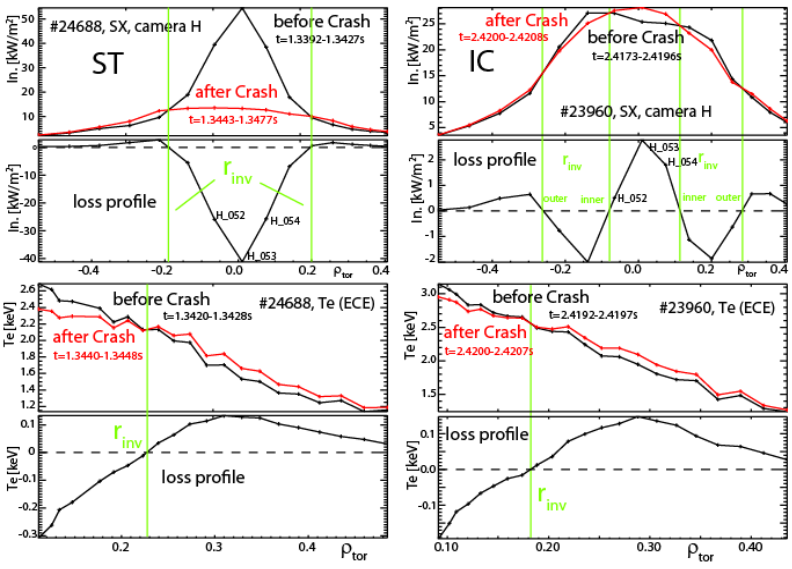

Figure 2: Profiles before and after crash and loss profile for SXR (intensity: line integrated emissivity) and T_e for a ST (left) and an IC (right). In SXR profiles ρ_{tor} is that of the flux surface tangential to the line of sight. The sign of ρ_{tor} is introduced artificially to distinguish between the two sides of the magnetic axis.

Figure 1 shows a change from normal peaked SXR profiles and sawtooth crashes (ST) to hollow profiles and ICs when central ECRH is switched on. Figure 2 shows the SXR and T_e profiles directly before and after a ST and an IC together with the loss profiles. T_e is

flattened during the crashes, leading to losses inside the inversion radius, r_{inv}, (approx. at q=1), and an increase outside. SXR close to the axis decreases during a ST but increases with an IC. (Note that the local emissivity is by far more hollow than the line integrals.). SXR loss profiles have approximately the same r_{inv} as T_e in the case of ST. For ICs they have two different r_{inv}, one inside, the other outside q=1. Both crashes have (m=1,n=1) precursors (m and n: poloidal and toroidal mode number) and their duration is similar. From these observations, ICs are likely to be normal ST with merely different initial condition - the hollow SXR profiles.

To study a wide range of discharges, a hollowness parameter, h, has been defined from the line integrated SXR data: The interpolated intensity values of one pinhole camera at ρ_{tor} = 0.1 (0.15 and 0.2) from both sides of the magnetic axis have been averaged and divided by the interpolated value at ρ_{tor} = 0 (magnetic axis). A local radiation profile which is flat inside q=1 results in still slightly peaked line integrated profiles, corresponding to a hollowness parameter, h, below one. After a ST, h at ρ_{tor}=0.1 is typically around 0.95, which was taken as threshold for hollow profiles. There are only few cases, in which hollow SXR profiles have been observed without ECRH: with hollow T_e profiles (after W accumulation and radiation cooling), with hollow n_e profiles (transiently during fast n_e increases starting from low n_e), and occasionally during W snakes [3] (discussed below). In all other plasmas with h ≥ 0.95, central ECRH was present. These discharges will be investigated in the following.

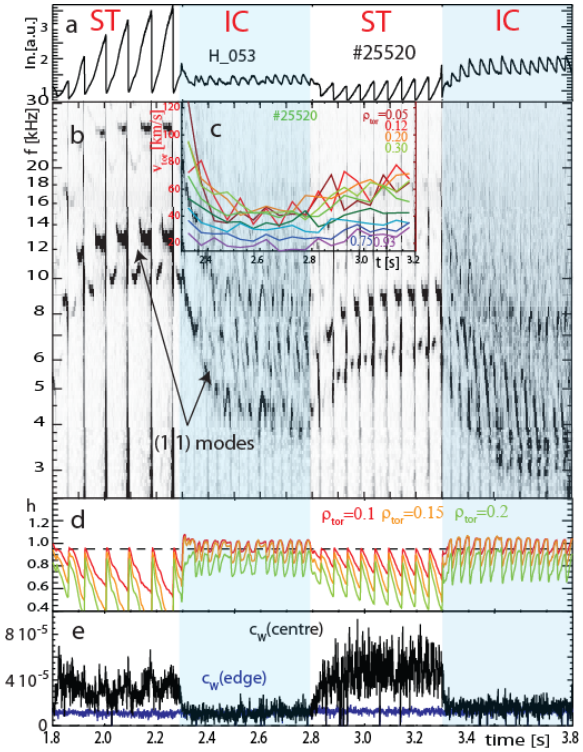

Figure 3: Time trace (a) and spectrogram (b) of a central SXR channel, toroidal velocities (c) from Charge eXchange Recombination Spectroscopy (CXRS), hollowness h (d) and W concentrations (e) [7]. Blue areas mark time ranges with central ECRH. The lower central c_W in ECRH phases indicates the prevention of W peaking with central ECRH [8]. The mode frequency (b) indicates the rotation velocity. Note the inverted crash signature of h compared to central SXR.

Both in L and H Mode discharges in ASDEX Upgrade, SXR profiles are hollow very often with central ECRH: the central SXR emissivity (unfolded) can be lower than the maximum by a factor of 5. In L Mode discharges with low n_e, occasionally hollow n_e profiles have been observed correlating with hollow SXR profiles. In H Mode, central n_e profiles are typically flat or slightly peaked, and T_e profiles are peaked. Therefore, hollow impurity density profiles must be responsible for the hollowness. Due to the W wall coverage, W is present in all ASDEX Upgrade plasmas. We therefore assume that the hollow radiation profiles are in most cases caused by hollow W density profiles.

Several ideas for the origin of the hollow impurity profiles are discussed in the following. In fast rotating plasmas, centrifugal forces become important especially for heavy, and hence supersonic, impurities, resulting in a poloidal asymmetry of the impurity density [4]. Rotation can also affect impurity transport ([5,6] and references therein). In the experiment, asymmetry of radiation profiles between high and low field side is observed in NBI heated plasmas, which gets more pronounced when the plasma rotates faster. This confirms that heavy impurities contribute significantly to the SXR radiation. However, figure 3 shows that the ICs occur only with central ECRH, where also the hollowness is increased, whereas the toroidal velocity is lower in this phase. Obviously, the effect of toroidal rotation on transport can not account for the hollow impurity profiles described here.

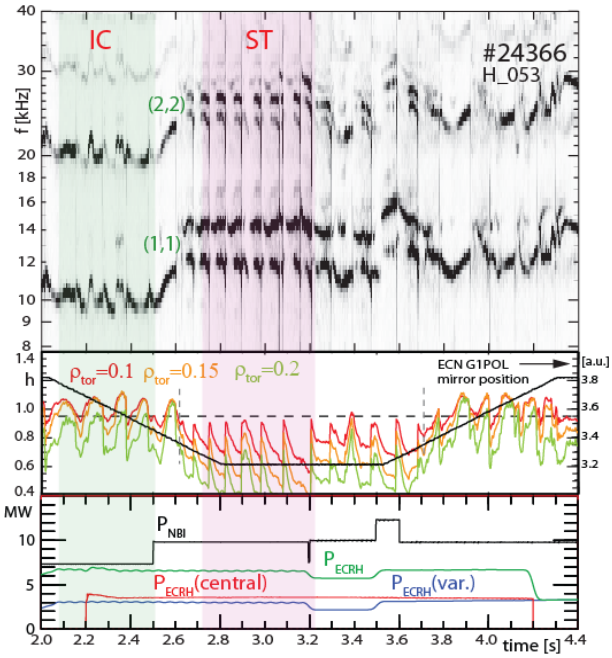

Figure 4: Spectrogram of central SXR, h and heating powers. Transition between peaked and hollow phases (grey vertical dashed lines) occur at the same mirror position of ECRH (var.). When (1,1) with higher frequency is strong, SXR profiles are peaked.

Mechanisms of outward convection of impurities have been suggested in the framework of turbulent transport theory, and indicate the possibility of hollow impurity density profiles in the presence of turbulence propagating in the electron drift direction [9].

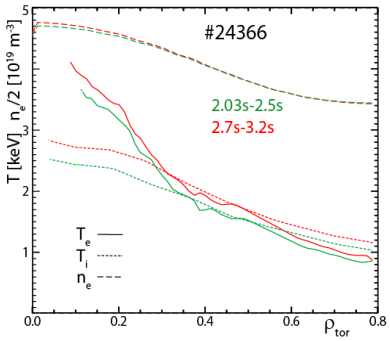

Figure 5: Electron and ion temperature and n_e time averaged during phases with strongly hollow and with normal SXR profiles (see figure 4). Temperatures rise due to an additional neutral beam at 2.5s.

T_e and T_i as well as their gradients are crucial for this model. Due to the presence of (1,1) modes, the existing codes are not applicable in the region where the outward convection is observed. However, Figure 5 shows that there is no significant difference in T_e and T_i profiles between phases with hollow and peaked SXR profiles (see figure 4).

Figure 4 shows a spectrogram of a discharge with central ECRH. The deposition of about half the ECRH power is moved with a steerable mirror during this time range from inside to just outside q=1, and back later. There are phases with strongly hollow and with clearly peaked SXR profiles. The change between them occurs roughly at the same mirror position, which corresponds to an ECRH deposition around q=1 ($\rho_{tor} \approx 0.17$). The reduction of ECRH power outside q=1 (3.2-3.5s) also modifies the hollowness. Clearly, the power and deposition distribution of ECRH plays a crucial role for hollow impurity profiles.

Peaking of SXR radiation around q=1 has been observed when W is strongly accumulated around the O-point of a magnetic (1,1) island, causing the typical signature of a W snake in

the SXR time traces [3]. Indeed, we always observe mode activity on the q=1 surface with hollow SXR profiles. Moreover, the (unfolded) radiation peak is close to q=1 and the hollow structure rotates with the (1,1) modes. However, the modes observed here have no snakelike character.

We often observe several q=1 modes, not only with ECRH or hollow profiles. Within our spatial resolution, these modes are at the same position, but can have significantly different frequencies. In figure 3, e.g, during phases without ECRH, a (1,1) mode occurs some time after a ST, while later in the sawtooth cycle a (1,1) mode with higher frequency dominates. Although we do not observe W snakes, there is often a striking correlation between central modes and hollow SXR profiles. In figure 4, e.g., the profiles are hollow only when there is no strong (1,1) mode with the higher frequency. Figure 6 shows another example: an (m=2,n=2) mode that occurs short time after ICs. During this mode the hollowness is increased rapidly. In the later phase of the crash cycle, the hollowness correlates well with the amplitude of the (1,1) mode with lower frequency.

Hollow central radiation profiles in the Soft X-ray range, which are probably attributed to hollow W densities, are observed regularly in discharges with central ECRH. Neither the effects of plasma rotation on transport nor turbulent transport in the presence of increased electron temperature gradients can explain the hollowness. Although there are usually no snakelike modes observed, the strong correlation between SXR profile shape and observed modes around q=1 suggests that these modes play a role for the hollow W profiles. Transport analysis will in any case be affected by the existence of central modes.

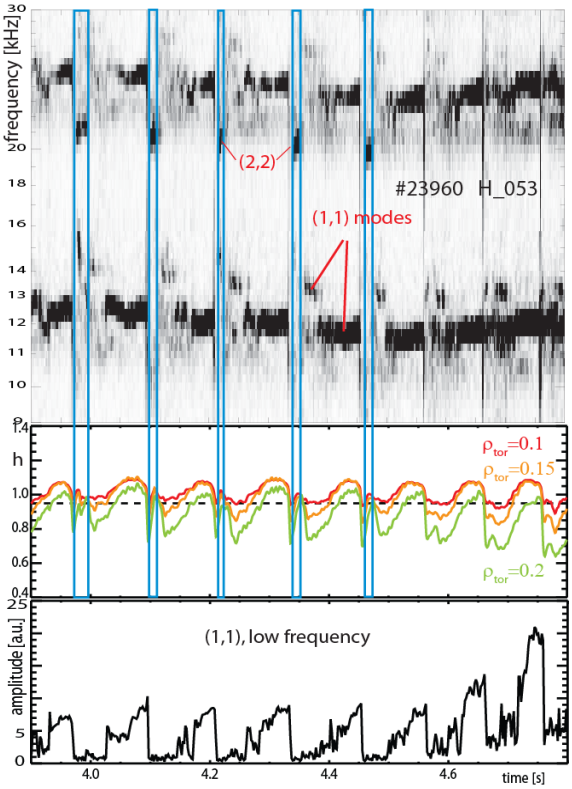

Figure 6: Spectrogram of central SXR channel, hollowness and amplitude of (1,1) mode with lower frequency. Blue rectagles mark existence of a (2,2) mode, during which hollowness is increased. At other times, h correlates well with the (1,1) amplitude.

In the future we will try to further characterize the q=1 modes in terms of radial structure, localization and systematics of their correlation with SXR profiles. Their occurrence with respect to fast particle distribution and other plasma parameters as well as the influence of heating scheme details will also be analyzed.

[1] Igochine, et al. IPP Report 1/338 (2010)

[2] Neu, et al, PPCF **49** (2007) B59

[3] Naujoks, et al, NF **36** (1996) 671

[4] Wesson, NF **37** (1997) 577

[5] McClements, et al, PPCF **51** (2009) 115009

[6] Camenen, et al, PoP **16** (2009) 012503

[7] Pütterich,et al, PPCF 50 (2008) 085016

[8] Wagner, et al, IEEE Trans. Plasma Sci. **37** (2009) 395

[9] Angioni, et al, PPCF 49 (2007) 2027